Chandrasekhar S. 1983 *The Mathematical Theory of Black Holes* (Oxford University Press, New York)
Cohen J. M., Gautreau R. 1979 *Phys. Rev.* **D19**, 2273
De Felice F. 1968 *Nuovo Cimento* **B57**, 351
Landau L. D., Lifshits E. M. 1973 *Teoriya polya* (Izd. Nauka, Moskva)
Misner C. W., Thorne K. S., Wheeler J. A. 1973 *Gravitation* (W. H. Freeman and Co., San Francisco)
Sharp N. A. 1979, *Gen. Rel. Grav.* **10**, 659
Stuchlík Z. 1981a *Bull. Astron. Inst. Czechosl.* **32**, 40
— 1981b, *Bull. Astron. Inst. Czechosl.* **32**, 366
Stuchlík Z., Bičák J., Balek V. 1989, in preparation (Paper III)
Zel'dovich Ya. B., Novikov I. D. 1971 *Teoriya tyagoteniya i evolyutsiya zvezd* (Izd. Nauka, Moskva)

SOME CHARACTERISTICS OF THE DEVELOPMENT AND EMISSIONS OF MAY 13, 1981 FLARE

L. Křivský[1]), V. E. Merkulenko[2]), L. E. Palamarchuk[2]) V. I. Polyakov[2])

[1]) *Astronomical Institute, Czechoslovak Academy of Sciences, 251 65 Ondřejov, Czechoslovakia*
[2]) *Sib. IZMIR AN, 664033 Irkutsk, USSR*

Received 16 September 1987, revised 24 October 1988

НЕКОТОРЫЕ ХАРАКТЕРИСТИКИ РАЗВИТИЯ И ЭМИССИЙ ВСПЫШКИ 13 МАЯ 1981

Выполнена комплексная обработка развития и эмиссий слабой протонной вспышки с γ эмиссией 13 мая 1981 г. Сравнивался ход эмиссии в Hα, Hβ, рентгеновской и радиоэмиссии в связи с изменениями производного поля радиальных скоростей в активной области со вспышкой. Особенно в тех местах при вспышке, где образовался небольшой вспышечный канал, были доказаны подъемные движения. Основное выделение энергии и ускорение частиц произошло в период 04 12—04 16—04 22 UT, по поправке на свет 04 04—04 14 UT.

The development and emissions of the weak proton flare of 13. V. 1981, with a γ-emission, have been treated comprehensively. The emissions in Hα, Hβ, the X-emission and radio emission were compared in connection with the changes in the derived field of radial velocities in the active region with the flare. The existence of ascending motions was proved particularly in that space near the flare, where a small flare channel had formed. The main energy emission and particle acceleration took place between 04 12 and 04 22 UT, with the main phase on 04 16; after correction on light between 04 04 and 04 14 UT.

Key words: solar proton flare: evolution in hydrogen lines, radio and X-emission, radial velocities

1. Development of the Flare

The flare of 13. V. 1981, importance 3B, originated in active region HR 17 644 (N 11, E 58), its maximum occurred at 04 18 UT. According to the classification of X-emission bursts its importance was X 1·5 (GOES satellite). Measurements made on the board the GMS satellite indicate that was connected with a weak proton emission; a burst of γ-emission was also recorded by the Hinotori satellite in the interval of 4·0–6·1 MeV (Yoshimori and Watanabe 1985).

The flare was observed with a coronograph at the Sajany Observatory (near Irkutsk) from 03 14 to 05 13 UT through an interference polarization filter in Hα, width 0·009 nm. The filtergrams in Hα and Hβ lines of the flare are shown in Figs 1a–f (for all Figs 1 see Plates 2 and 3. The flare was simultaneously photographed in the centre of the Hα line (Figs 1g–h). The active region is depicted in Fig. 2. The emission variations at the centre of the Hβ line (Fig. 5) correspond to the flare nodes marked in Fig. 2. With regard to these curves, the development of the flare can be divided into three stages:

a) the initial stage, 03 40–04 12 UT, prior to the main flare outburst corresponds to the "preflare" (Bumba and Křivský 1959). The emission radiated in nodes 4, 7 and 8;

b) the maximum stage, 04 12–04 34 UT, characterized by an increase in the radiation of nodes 3, 4 and 9. At the same time, the brightness of nodes 1, 2, 5, 6

gradually grew near the spot of magnetic type δ (with both polarities close together in one penumbra);

c) the decay stage of the flare, 04 34 – 05 13 UT. At this time the flare emission penetrated and above the spot at the centre of active region and expanded westwards.

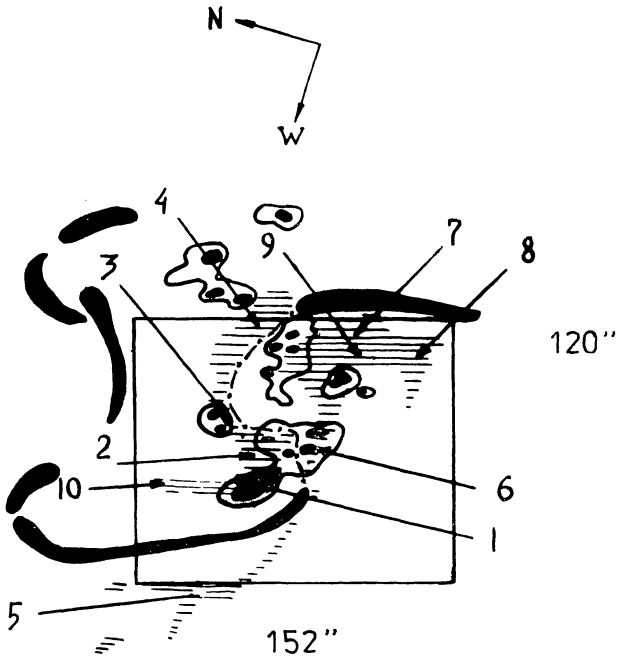

Fig. 2. Schematic representation of the observed flare (hatched) in the active region with spots (May 13, 1981, HR 17 644) with numbering of the principal flare nodes. The absorption filaments are in black. Dot-dashed line — divide of magnetic polarities. The area of the rectangle shows the observed and treated area in Figs. 3 and 7.

A synthesis of the photographs in Hα and Hβ (Fig. 1) shows that, with regard to dynamics and topology, the flare consisted of two different systems: the first system represents the northern, almost stationary flare ribbon (with nodes 3, 4), the second system is the southern ribbon near and southwards of the spot (with nodes 7, 8, 9). This second system display bifurcation of the ribbon prior to 04 16 UT (Fig. 1d, Hβ +0·025, 04 16 UT). The remaining traces of this bifurcation and prolongation of the flare ribbon westwards could still be seen in Hβ (Fig. 1f) at 04 56 UT. This space can be identified with the described Y-phase (Křivský 1963), i.e. with the space of maximum energy outflow at the start of explosive phase in the form of accelerated particles (cf. also Section 7).

2. X-emission of the Flare

Figure 6a shows the X-emission in there ranges, from 17 to 152 keV, as reported by Tsuneta et al. (1984) on the basis of the Hinotori satellite records; beginning of the burst at 04 12, maximum at 04 15 30 UT. The hard emission (identical with explosion phase) did not display an impulsive character.

Figure 1d shows two-dimensional drawing of the image of the flare obtained in the 10 – 20 keV X-emission in the form of an extensive arc or loop (Tsuneta et al. 1982). The maximum of this emission is at the apex of the loop-system; such loops are, as a rule, at heights of about 50 000 km. Both bottom outer parts of this loop formation point towards nodes 8 and 9 (Fig. 2), this anchoring is identical with the locations at which the flare ribbon (=flare channel) bifurcated. In this space (which is always typical for ribbon bifurcation) loops originated, radiating in the X-emission; this formation does not agree with the position of the northern anchoring of the absorption loops (in Hβ, Fig. 1e, f) or of the emission loops in Hα (*h*); these loops are anchored more to the side, beyond the boundary of the northern emission flare ribbon, namely in the region of spots and small spotlets. Both loop systems were clearly neither spatially nor physically connected, and evidently formed at different times.

3. Radio Emission

Figure 6b shows the variations of radio emission on 10·2 cm (2950 MHz), 31·5 cm (950 MHz) and 46·1 (650 MHz), (Melnikov et al. 1983). The advance of the maximum of the hard X-emission relative to the maximum on 10·2 cm is 4·0 – 4·5 min. Maximum is evidently connected with the development of the secondary process. The lag of maximum of the radio emission 10·2 cm in relation to the maximum of brightness in Hβ is about 2·0 – 2·5 min.

4. Changes of the Flare Brightness

The brightness maps represent half the sums from the Hβ-wings +0·026 and Hβ −0·029 nm for times 04 16 43 and 05 03 20 UT and are shown in Figs 3 and 4 (see Plate 1). The spot areas are hatched. The flare ribbons are shown by dashed lines. The changes in flare emission (the individual flare nodes are marked by numbers in Fig. 2) are shown in Fig. 5. The ratio of the node brightness to the background is on the vertical axis, the time on the horizontal.

Figure 6d shows the curve of emission change in the centre of the Hβ-line obtained by average of

emission curves of all flare nodes shown in Fig. 5 (positions of nodes see at the Fig. 2).

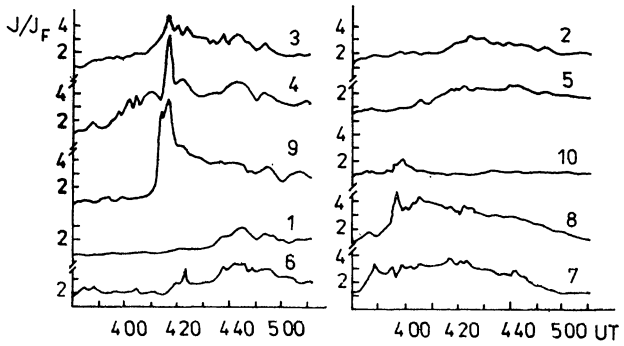

Fig. 5. Curve of change in flare node brightness marked by numbers and positions according to Fig. 2. The vertical axis shows the ratio of the flare node brightness to the background brightness, J/J_F; the horizontal the time.

5. Field of Radial Velocities in the Space around the Flare and Their Relation to the Radio Emission

A. *Gradual Changes in Velocities During the Flare*

The filtergrams Hβ +0·026 nm and Hβ −0·029 nm were used to calculate 54 maps of the field of velocities of 120″ × 152″ in area (Fig. 2). The mean interval between the maps was 1·5 min. The method of processing the filtergrams is described in the paper of Stepanov et al. (1981).

Only two velocity maps for 04 16 43 and 04 20 30 UT are shown in Figs. 7 and 8 (see Plate 1). The velocity variations in the active region as a whole at the time of the flare can be derived from variations $\tilde{V}_+$ (positive radial velocity – the plasma is moving away from the observer) and $\tilde{V}_-$ (negative radial velocity – the plasma is moving towards the observer). They are shown in Fig. 6c and are the result of averaging over the whole studied area outside the spot and flare ribbons (the calculation of the velocities in spot and flare ribbons locations are subject to errors for various reasons). One can also see the fluctuation of radial velocities display periodicities of about 5 mins.

In order to obtain an image of the slower changes of velocities the obtained velocities were averaged in the intervals 03 40 – 04 06 UT (in the initial stage of the flare development), 04 13 – 04 33 UT (flare maximum), and 04 34 – 04 47 UT (flare decay). Figures 9 – 11 (see Plate 4) show these maps in the intervals mentioned. The regions of negative velocities (towards the observer, i.e. the ascent) are hatched. The following peculiarities of the velocity fields can be observed beyond the flare ribbons:

1. the dividing line between the velocities of opposite sense is near the dividing line of polarities (towards the zero line)
2. the positive velocities (away from the observer, i.e. decrease) show, on the average, a larger amplitude than the negative ones
3. regions of high negative velocity values were observed in the neighbourhood of the spot of magnetic type δ, which evidently indicates the rise of plasma and magnetic fields above the photosphere
4. a significant expansion of the area with negative velocities occurs in the whole active region.

B. *Velocity and Brightness Variations During the Flare Radio Emission*

A survey of the variations in the velocity field over the whole active region can be obtained from the variations of the flux of positive $\tilde{V}_+ = \sum V_+ S_+$ and negative $\tilde{V}_- = \sum V_- S_-$ radial velocity where S_+ and S_- are the observed regions of positive and negative velocities in the area studied. Curves $\tilde{V}_+$ and $\tilde{V}_-$ are in Fig. 6. The comparison with the radio emission flux curves implies that the individual peaks on 21·5 cm roughly agree with the variations of the radial velocities with a period of about 5 min in the initial phase of the flare.

6. Results

Figure 2 show the dividing line of polarities of the magnetic field (dot-dashed line). In the same figure are indicate the flare ribbons at the time of flare maximum (hatched). One finds that nodes 1, 2, 3, 4 and 10 are in the region of S-polarity, and nodes 5, 6, 7, 8 and 9 in the region of N-polarity. By analysing the flare node brightness curves one can determine a several systems of flare loops and conspicuous changes in several flare fields:

a) node 8 (Fig. 1e, h, Fig. 2, Fig. 5) is bridged by coronal loops (in absorption Hβ Fig. 1e, in emission Fig. 1h) with spots 7 and 5. The behaviour of the brightness of node 8 different from the other flare nodes. At 03 57 UT an marked increase of brightness in Hα was observed in this position (start of preflare). This outburst was simultaneously connected with an event in the velocity fields as well as with gradual emission in the radio range (Fig. 6b).

b) according to the 10 – 29 keV X-emission the apexes of coronal arcs began to radiate at 04 01 30 UT (Tsuneta et al. 1984); the arcs point away from node 8 and return to the vicinity of nodes 7 and 9, (Fig. 1d),

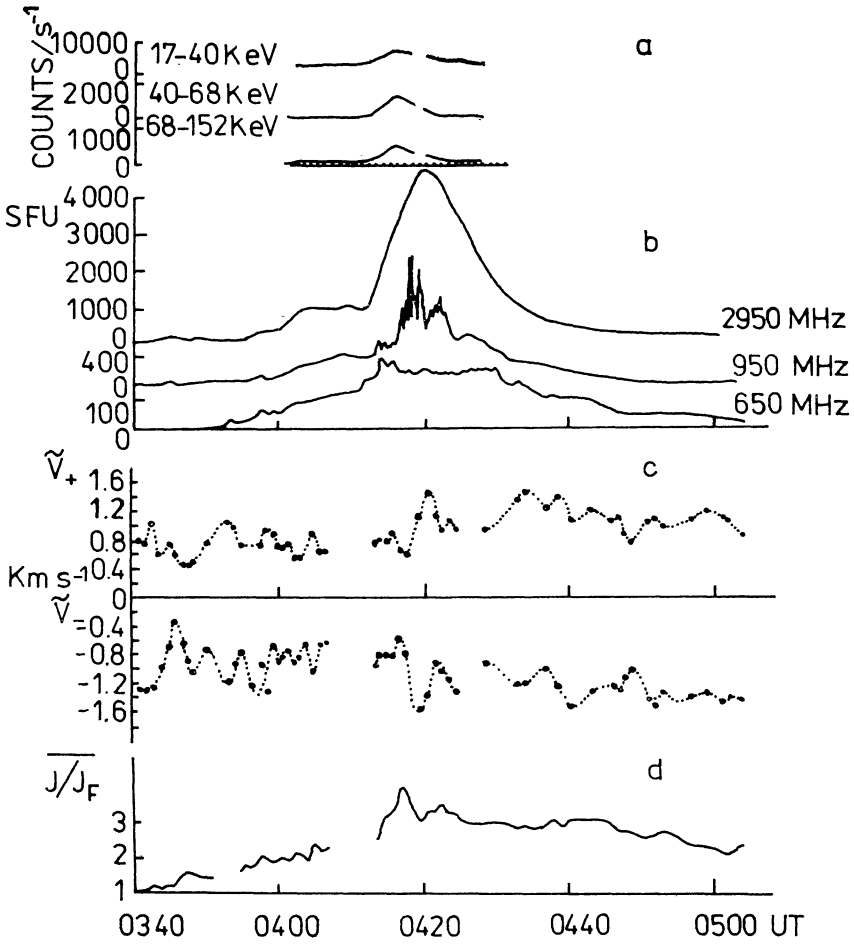

Fig. 6. a) Change of the X-emission in three channels measured by the satellite (Tsuneta et al. 1984); b) changes of the radio emission on three frequencies: 2950 MHz — 10·2 cm, 950 MHz — 31·5 cm, and 650 MHz — 46·1 cm (Melnikov et al. 1983); c) averaged flux of positive radial velocity $\tilde{V}_+$ and negative velocity $\tilde{V}_-$ in the active region at the level of the chromosphere; d) $\overline{J/J_F}$ brightness variation at the centre of the Hβ line averaged from all flare nodes (Fig. 5). Position of the nodes at the Fig. 2.

and the preflare emission continues to develop inclusive of radio emission (Fig. 6). This system is most likely connected with the preparatory stage of the physical situation for the subsequent main flare.

c) the maximum stage of flare development coincides with the marked increase in the brightness of node 9 (Fig. 2), where the already existing coronal loops in Hα and Hβ near spots 5, 6, and 7 are anchored (Fig. 1c, e, h). According to the Hinotori satellite data, the maximum outburst in the X-emission at 04 15 30 UT is 30 seconds in advance of the maximum Hα-brightness outburst of node 9.

d) nodes 1 and 6, 2 and 5, 4 and 7 (Fig. 2) are evidently connected with the low-lying flare loops forming the flare complex. Nodes 4 and 7 can be combined on the basis of simultaneous course of brightness in the evolution of the preflare and whole flare. The intensive bursts of node 4 at 04 17 20 UT is evidently connected with part of the inner short coronal loops being connected to this node from the small flare channel (nodes 7, 8, 9, Fig. 1h).

e) attention has to be drawn to the existing bonds between both main flare ribbons: this involves the apparent bridging which evidently formed at the time of preceding flares and which continued (Fig. 1g).

7. Discussion and Conclusions

The flare of 13. V. 1981 had a preflare stage perceptible after 03 40 and characterized by a gradual brightening; the phenomenon can be denoted as a preflare particularly after 03 57 UT; the main explosive phase formed after 04 12.

It may be said that this flare partly differed from the typical scenario of proton flares (Křivský 1963, 1977). As regards the flare of 13. V. 1981 and even before it, there existed a system of arcs or loops

with a reserve a coronal energy from the time of the past flares to the beginning of the main explosive phase of the flare (after 04 12 UT), and the new system of loops with high temperatures and a strong X-emission originated in a rather small space, where the flare ribbon bifurcated and a new flare channel was formed (in the vicinity of nodes 7, 8, 9). In the very same space both previous loop anchorings in the X-emission can be observed as documented by their two-dimensions photograph (Fig. 1d). The space of their anchoring corresponds in time with the subsequent main outburst in the Hα emission, with the formation of two new ribbons and their separation (phase Y) in this rather small space, and, what is most important, with the outburst of the X-emission in three channels from 17 to 152 keV. This critical period, as also indicating by the onset of the radio emission bursts, reveals the physical process, responsible for the prime explosive energy emission including the emission of protons. It is possible that the previous extensive loop system, also pointing from the critical space to the more distant spots, was saturated by energy, but was of secondary importance.

It is also interesting to note the transverse bonds between the two main emission ribbons of the flare, revealing the past flare activity, which can be seen in the absorption and in weak emission in the Hα photograph at 04 37 UT (Fig. 1g); this loop formation (the earlier flare channel) was the principal source of energy amission in the past. In the flare of 13.V. 1981 after ~04 12 UT, the process was analogous, but connected with a different area (eastward of spot 3 at Fig. 1c, cf. Fig. 10, in the vicinity of node 9 – Fig. 2) where a new magnetic field of opposite direction probably rose in the narrow space. This interpretation also agrees with analogous case of large flares observed near the limb of the disk, where secondary processes connected with radiation in Hα (or Hβ) reveal, under reduced temperatures in the marginal sections of the magnetoplasmic loop formations, the principal areas and processes of the flare channel connected with radiation of harder and hard ranges of the X-emission (Křivský et al. 1987).

The localization of the primary physical areas is also disclosed in such flares, by the mm and cm radio emissions (provided their images exist) which, as a rule, only last during the time of the hard X-emission, and this is logical from the point of view of physical interpretation. Radio emissions of the wavelengths > 6 cm come from energetically subsidiary spaces of developing and ascending loops, viz from their different heights, where the magnetic tubes are filled by electrons of energies between 100 and 150 keV. In these later stages (after the explosive phase of the flare), the plasma may flow from one end of the loops, to the other, at a time the primary processes and instabilities in the loops, particularly in the anchoring areas and apexes, have already decayed, and the development of secondary processes with soft X-emissions and lasting Hα emissions follows. The mentioned overflow of plasma in the system of flare loops may be the consequence of different pressure gradients along the loops due to different temperatures at their ends. This process may then interfere with the most diverse loop systems which extend to larger distances at the flanks from the flare channel itself, in which magnetoplasmic instabilities have been triggered and fast particles accelerated (including energetic protons).

The main energy emission (and acceleration of particles) occurred within the interval 04 12 – 04 22 UT particularly at about 04 16 UT (in agreement with the occurrence and behaviour of the hard X-emission), and further at the time of the bifurcation of the flare ribbon near spot 3 at about 04 16 (cf. Fig. 1c, Hβ +0·063). In reality the ejection of fast particles was realized 8 min earlier (owing to the correction on light, that means at 04 04 – 04 14). In Fig. 1f (Hβ 04 56 UT) only the remnants of this bifurcation are visible (the width of the channel attained 53 000 km).

The spectral continuum in the bifurcation of Hα ribbons (in the region of new creation of flare channel) at about 04 11 45 (Hiei et al. 1982) represents a further argument for locating the triggering of the main explosive process in the flare, of the maximal release of energy and particles acceleration. It is approximately in the bright flare knot 9 in our notation (Fig. 2), near spot 3 (Fig. 1c).

Numerous cases in the past have shown that of the flare, or only its smaller part, displays bifurcation of the ribbon (i.c. the forming of a flare channel in consequences of magnetoplasmic instabilities), fast protons are recorded in the vicinity of the Earth. If this bifurcation (channel) occupies a small space and the width of the channel is not large, the number and energy of protons are not large either, regardless of the class of importance of the whole flare in the Hα line. This was also the case with the flare we have studied (Yoshimori and Watanabe 1985).

Important is the observation of the ascending plasma motion (apparently with frozen-in magnetic fields) in the space near the flare ribbons and near the flare channel (knots 7, 8, 9, Fig. 2), in particular during the explosive phase of the flare.

REFERENCES

Bumba V., Křivský L. 1959 *Bull. Astron. Inst. Czechosl.* **10**, 221

Hiei E., Tanaka K., Watanabe T., Akita K. 1982 *Hinotory Symp. on Solar Flares* (Inst. of Space and Astronaut. Sci., Tokyo), p. 208

Křivský L. 1963 *Nuovo Cimento X*-**27**, 1017

— 1977 Solar Proton Flares and their Prediction, *Publ. Astron. Inst. Czechosl. Acad. Sci.* No 52

Křivský L., Fárník F., Sudová J., Valníček B. 1987 Proc. 10th Europ. Reg. IAU Meeting Vol. 1 (Eds L. Hejna and M. Sobotka), *Publ. Astron. Inst. Czechosl. Acad. Sci.* No. 66, p. 233

Melnikov V. F., Nefedev V. P. Podstrigach T. S., Prokudina V. S., Potapov N. N., Smolkov G. Ya. 1983 *Publ. Debrecen Heliophys. Obs.* **5**, 167

Stepanov V. E., Ermakova L. V., Merkulenko V. E., Palamarchuk L. E., Polyakov V. I., Klochek N. V. 1981 *Issled. po geomagn. aeronomii i fiz. Solnca* (*Irkutsk*), Nauka Moskva, **56**, p. 98

Takahura T., Ohki K., Tsuneta S., Nitta N., Makishima K., Muraki T., Ogawa Y., Oda M. 1982 *Hinotory Symp. on Solar Flares* (Inst. of Space and Astronaut. Sci. Tokyo), p. 142

Tsuneta S., Takakura T., Nitta N., Ohki K., Tanaka K., Makishima K., Murakami T., Oda M., Ogawara Y., Kondo I. 1984 *Astrophys. J.* **280**, 887

Yoshimori M., Watanabe H. 1985 *19th Inter. Cosmic Ray Conf.* (USA 1985), NASA, SH **4**, 90

THE PERSEUS FLASHER: INVESTIGATION USING ONDŘEJOV PLATES

J. Borovička, R. Hudec

Astronomical Institute, Czechoslovak Academy of Sciences, 251 56 Ondřejov, Czechoslovakia

Received 3 November 1987

ВСПЫХИВАЮЩИЙ ИСТОЧНИК В ПЕРСЕЕ: ИССЛЕДОВАНИЯ НА ПЛАСТИНКАХ ОБСЕРВАТОРИИ ОНДРЖЕЙОВ

Обсуждается реальность вспыхивающего источника в созвездии Персея, который был обнаружен как источник частых и коротких оптических всплесков. Были обработаны пластинки из коллекции обсерватории в Ондржейове. Источник отсутствует на симультанных по времени пластинках для 4 явлений а также на пластинках преставляющих собой 1 350 часов наблюдения. Показано, что заключения Катза и др. (1986) должны быть ошибочными и что источник не является реальным астрофизикальным объектом. Обсуждается наблюдаемая частота всплесков и показано, что она значительно больше чем оценка этой величины от оптических явлений от спутников. Предложено объяснение, что основная часть (>50%) наблюдаемых всплесков физиологического происхождения.

The reality of the Perseus Flasher (PF), which was found as a source emitting frequent and short optical flashes, is analysed. The results based on investigating of the Ondřejov Observatory plate collection (no confirmation on time-correlated plates for 4 events; no object on plates representing a total of 1350 hours of exposure) indicate that the conclusions drawn by Katz et al. (1986) must be in error and strongly support the nonastrophysical origin of the object. On the other hand, we argue that the reported PF frequency is considerably higher than the estimated frequency of background flashes, and difficulties exist in the interpretation of the PF as a satellite glints phenomenon. We suggest another plausible explanation, namely that a large part (>50%) of the optical flashes, reported as PF, are physiological in origin.

Key words: Perseus flasher — Ondřejov plate collection

1. Introduction

The Perseus Flasher (PF) was found by Katz et al. (1986) as a probable astrophysical object which frequently (every 12 h in the mean) emits bright ($\leqq 2^m$) and short ($\leqq 1$ s) optical flashes of large ($>19^m$) amplitude.

On the other hand, the results published by other groups does not confirm these findings:

Hudec et al. (1986) reported no object within 1080 hours of photographic exposure, Vanderspek et al. (1986) no object within 70 hours of CCD exposure and 1700 hours (from this amount however only 700 hours were sensitive enough to detect 1-sec flashes fainter than $-0{\cdot}5^m$) of photographic exposure.